Volume: 1 Issue: 3 Pages: 29-39

Analysis of Thermodynamic Functions, Non-Linear Optical Properties and UV-Vis Spectra of 2-Chloro-3-Hydroxy-4-Methoxybenzaldehyde by Quantum Chemical Calculations (Hartree-Fock and Time Dependent Density Functional Theory)

[*1] Dr. Rajesh Kumar

[*1] Assistant Professor, Department of Physics, Government Degree College, Kursanda, Hathras, Uttar Pradesh, India.

Article Info.
E-ISSN: 2583-6528
Impact Factor (SJIF): 3.477
Available online:
www.alladvancejournal.com

Received: 23/Nov/2022
Accepted: 26/Dec/2022

***Corresponding Author**
Dr. Rajesh Kumar
Assistant Professor, Department of Physics, Government Degree College, Kursanda, Hathras, Uttar Pradesh, India.

Abstract
This work presents the analysis of compound 2-Chloro-3-Hydroxy-4-Methoxybenzaldehyde (abbreviated as 2,3,4-CHMB). The HF and DFT/B3LYP methods were used to optimize the molecular geometry in the ground state and calculate thermodynamic functions, non-linear optical properties and UV-vis spectra of the title molecule using 6-31+G(d,p) and 6-311++G(d,p) as basis sets, respectively. The thermodynamic functions of the title molecule were computed at different temperatures. Using the same basis sets, the HF and TD-DFT methods were also used to calculate the investigated molecules' electric dipole moment, polarizability, and first hyperpolarizability values. In the 200–450 nm range, the UV spectra were experimentally recorded in different solutions (acetone, diethyl ether, and CCl4 as solvents). The theoretical scaled values are compared with experimental values. The measured experimental results were found to be in good agreement with the theoretical results.

Keywords: HF, TD, DFT, B3LYP, UV-Vis, NLO

Introduction

The simplest representative of the aromatic aldehydes known as benzaldehydes, is found in peaches, apricots, cherries, and almond. It occurs naturally as the glycoside amygdalin, which is a sugar derivative of the cyanohydrin of benzaldehyde that is found in bitter almonds. Although benzaldehyde is mostly known as an artificial essential oil of almond, it has numerous other applications, including the production of flavorings, dyes, fragrances, cinnamic and mandelic acids, and solvents. The use of benzaldehyde in the agricultural and health sectors has evolved recently. Benzaldehyde is utilized as an anticancer agent and as a pesticide. It works as a bee repellent when honey is being harvested. The chemical and biological significance of benzaldehyde and its derivatives has drawn attention [1-5]. Numerous spectroscopic investigations have been carried out on benzaldehyde and substituted benzaldehydes. Spectroscopists have been curious about mono-, halo-, methoxy-, and ethoxy-substituted benzaldehydes. Due to their ability to resist bacterial infections, viruses, cancer, and fungi, benzaldehyde and its hydroxyl derivatives are of great interest. The oxidative property of hydroxybenzaldehyde is amazing because it promotes leptin signaling and reduces fat formation in adipose tissues by triggering fat oxidation. The intracellular coagulation of cytoplasmic constituents caused by hydroxybenzaldehyde either inhibits cell growth or leads cell death. Numerous spectroscopic analyses of halogen and methyl substituted compounds have also been published in the literature [6–15]. N. Sundaraganesan *et al.*,[21] have studied the spectra of 3,4-dimethylbenzaldehyde. V. Krishna Kumar and V. Balachandran have reported vibrational spectra of 2-hydroxy-3-methoxy-5-nitrobenzaldehyde [22]. Likewise, several spectroscopic studies on di- and tri-substituted benzaldehydes have been reported [17–22].

In recent years, non-linear optic (NLO) materials have gained attention due to their potential uses in optoelectronic fields such dynamic image processing, optical communication, optical computing, and optical switching [23, 24]. Organic materials exhibit several remarkable non-linear optical features because of their strong molecular

hyperpolarizabilities. Numerous organic, inorganic, and organometallic molecular systems have been investigated for their NLO activity [23, 25].

It is apparent that systematic investigation of structure and vibrational assignments using ab initio and density functional theory (DFT) calculations has not been carried out on halogen and methoxy substituted benzaldehydes. The UV-vis analysis of 2-Chloro-3-Hydroxy-4-Methoxy-benzaldehyde (2,3,4-CHMB) and quantum chemical calculations have not yet been reported, as far as we are concerned. Due to the lack of sufficient information in the literature, we conducted this theoretical and experimental vibrational spectroscopy study based on the molecule's structure to provide an accurate assignment. Consequently, we have conducted a spectroscopic analysis of 2,3,4-CHMB.

In the present investigation UV spectrum was measured in different solvents (Acetone, Diethyl Ether, and Carbon Tetra Chloride). The excitation energy, wavelength corresponds to absorption maxima (λ_{max}) and oscillator strength are calculated by Time-Dependent Density Functional Theory (TD-DFT) using B3LYP/6-31+G(d,p) and B3LYP/6-311++G(d,p) basis sets. The calculated HOMO and LUMO energies show that charge transfer occurs within the molecule. The electric dipole moment, polarizability and the first hyperpolarizability values of the investigated molecule were also calculated using HF and DF methods with same basis sets. The experimental and theoretical values of thermodynamic parameters at different temperatures are also tabulated.

Experimental Details

The compounds under investigation 2,3,4-CHMB in solid form were purchased from Sigma–Aldrich Chemical Pvt. Ltd., Germany with a claimed purity of 99%, and used directly without additional purification. The 2,3,4-CHMB UV/Vis absorption spectra was recorded at IIT Roorkee using a Perkin Elmer Lambda-25 UV/Vis spectrometer at room temperature. The UV-vis spectra of 2,3,4-CHMB were measured in several solvents, namely carbon tetra chloride, diethyl ether, and acetone in the 200–500 nm range.

Computational Details

All of the quantum chemical calculations have been carried out at HF and DFT (B3LYP: the Becke's three-parameter hybrid method with the Lee, Yang, and Parr correlation functional) methods using the Gaussian 09 program with the 6-31+G(d,p) and 6-311++G(d,p) basis sets [26]. The optimized structural parameters have been evaluated for the calculations of vibrational frequencies by assuming C_s point group symmetry. The HF and DFT methods were also used to calculate the non-linear parameters (dipole moment, polarizability, and first order hyperpolarizability) using the same basis sets. The electronic absorption spectra for optimized molecule calculated with the time dependent density functional theory (TD-DFT) at B3LYP/6-31+G(d,p) and B3LYP/6-311++G(d,p) levels. The electronic absorption spectra for the optimized molecule were computed employing the time dependent density functional theory (TD-DFT) at the B3LYP/6-31+G(d,p) and B3LYP/6-311++G(d,p) levels.

Result and Discussion

Molecular Geometry

The optimized structural properties of 2,3,4-CHMB, computed using ab initio HF and DFT-B3LYP techniques with the 6-31+G(d,p) and 6-311++G(d,p) basis sets, are shown in table 1 in accordance with the atomic numbering scheme presented in figure 1. As all carbon atoms in the benzene ring are sp^2 hybridized and having uniform bond lengths and angles, the substitution of hydrogen in the benzene ring causes a perturbation in the valence electron distribution of the molecule, subsequently modifying its chemical and physical properties. The angular variations in benzene ring geometry showed sensitivity as an indicator of the interaction between the substituent and the benzene ring. The ring's bond length has also exhibited characteristic variation, yet it has been slight and less noticeable than the angular changes. Since the crystal structure of the title compounds is not available till now, the optimized structure can be only be compared with other similar systems for which the crystal structures have been solved [21,22]. Since the title compounds' crystal structure is currently unknown, the optimized structure can only be compared to other systems that are similar and have known crystal structures.

According to the literature on ab initio and DFT methods, bond lengths, especially CH bond lengths, are overestimated by DFT methods and underestimated by HF methods. For the 2,3,4-CHMB molecule, this theoretical pattern is also observed. With values from the crystallographic literature, these optimized parameters are a little bit overestimated. It is discovered that the B3LYP calculation yields higher values for the aromatic C–C bond distances of 2,3,4-CHMB than the HF calculation. The length of the carbon-carbon bonds varies in benzene. The six C–C distances differ only slightly from one another. But knowing that electronegative substituents on benzene rings tend to reduce the lengths of adjacent C–C bonds, we suggested that the bond lengths C1–C2, C3–C4, C1–C6, and C5–C6 were approximately equivalent, while the bond lengths C2–C3 and C4–C5 were shorter than the others for 2,3,4-CHMB. The C–H aromatic bond distances follow an identical trend, with relatively longer distances in B3LYP. The C–Cl bond length is nearly identical for all B3LYP basis sets. The C–Cl bond length reveals a significant increase when substituted for C–H. This occurrence has been observed even in derivatives of benzene [27]. The C–Cl bond length are found 1.752 A^0 (B3LYP) and 1.739 A^0 (HF) by using 6-311++G(d,p) and 1.752 A^0(B3LYP) and 1.738 A^0 (HF) by using 6-31+G(d,p) for 2,3,4-CHMB. C.S. Hiremath *et al*., [4] calculated this bond length as 1.751 A^0 (B3LYP/6-311G*) and 1.738 A^0(HF/6-311G*) for 3-Chloro-4-Methoxybenzaldehyde using force field calculations, the experimental value of the C–Cl bond for the same compound given by them is 1.734 A^0. This bond length was also observed as 1.735–1.744 A^0 range for similar molecules [28-33]. The bond angles determined by different methods exhibit similar patterns to the significant difference in bond lengths. The CCC angle at the chlorine substitution position in the ring is significantly larger than the others. The other CCC angles are nearly 120^0. The HF and DFT calculations also show a shortening of the angle C3-C2-Cl12 for 2,3,4-CHMB and an increase of the angle C1-C2-C3 for 2,3,4-CHMB from the normal 120^0 at the C2 position, indicating the Cl group's repulsion to the phenyl ring. Despite some discrepancies between our values and the literature data, the optimized structural parameters effectively replicate the literature findings and serve as the foundation for subsequent discussion.

Thermodynamic Functions

The thermodynamic variables of 2,3,4-CHMB are provided in Tables 2 and 3. The computed thermodynamic parameters for

2,3,4-CHMB utilizing HF and B3LYP with the 6-31+G(d,p) and 6-311++G(d,p) basis sets are given in table 2. Entropy means a measure of a system's disorder. The process of vaporization is associated with an increase in system entropy [34]. As temperature rises, entropy also increases, as demonstrated in table 3 for the molecule being examined. These values of thermodynamic functions are plotted as a function of temperature.

Figure 2 illustrates variations in free energy, enthalpy, and entropy functions with temperature for 2,3,4-CHMB. The study's results indicate that free energy, enthalpy, and entropy consistently rise with temperature, whereas heat capacity initially increases with temperature and thereafter remains nearly constant beyond a certain temperature [33,35]. At low temperatures, only translational motion contributes; however, as temperature rises, rotational and vibrational motions become excited [36-39]. Beyond a specific temperature threshold (approximately 1000 K), molecular motion ceases to increase, resulting in a nearly constant heat capacity. These figures indicate that at very high temperatures, the effects of anharmonicity become significant, resulting in an inaccurate representation. The various colored points depicted in the figure are utilized solely for the comparison of values of distinct thermodynamic potentials at corresponding temperatures. These figures demonstrate that the effect is negligible at temperatures as high as 1000K for free energy. The statistical computation of entropy is significantly less reliant on vibrational data than the other thermodynamic functions because, in the case of entropy at very high temperatures, the vibrational contribution is very small in comparison to other contributions. For similar molecules, previous researchers have reported similar trends of thermodynamic function variation with temperature [40-41].

NLO Properties

Based on the finite-field approach, HF and DFT are used to calculate the dipole moment μ, polarizability α, and second-order polarizability or the first hyperpolarizability β using the 6-31+G(d,p) and 6-311++G(d,p) basis sets. To compute the total static dipole moment magnitude μ, the mean polarizability α, the polarizability anisotropy Δα, and the mean first hyperpolarizability β_{Total}, the required complete equations using the *x, y, z* components from Gaussian 09W output are as follows:

The dipole moment $\mu = \sqrt{\mu_x^2 + \mu_y^2 + \mu_z^2}$

The mean polarizability and anisotropy of polarizability respectively are defined by

$$\langle\alpha\rangle = \frac{1}{3}(\alpha_{xx} + \alpha_{yy} + \alpha_{zz})$$

$$\Delta\alpha = \frac{1}{\sqrt{2}}\left[(\alpha_{xx} - \alpha_{yy})^2 + (\alpha_{yy} - \alpha_{zz})^2 + (\alpha_{zz} - \alpha_{xx})^2 + 6(\alpha_{xz}^2 + \alpha_{xy}^2 + \alpha_{yz}^2)\right]^{\frac{1}{2}}$$

the mean first-order hyperpolarizability β_{Total} is defined as

$$\beta_{Total} = (\beta_x^2 + \beta_y^2 + \beta_z^2)^{\frac{1}{2}}$$

where

$$\beta_x = \beta_{xxx} + \beta_{xyy} + \beta_{xzz}$$
$$\beta_y = \beta_{yyy} + \beta_{xxy} + \beta_{yzz}$$
$$\beta_z = \beta_{zzz} + \beta_{xxz} + \beta_{yyz}$$

The computed dipole moment values, including all components, are presented in Table 4. The dipole moment values for 2,3,4-CHMB were found to be 6.05 Debye (B3LYP/6-311++G(d,p)), 6.11 Debye (B3LYP/6-31+G(d,p)), 5.75 Debye (HF/6-311++G(d,p)), and 5.79 Debye (HF/6-31+G(d,p)). Using all methods, the value of dipole moment for component μ_x is highest and for component μ_y is lowest for 2,3,4-CHMB.

Atomic units (a.u) is used to report the polarizabilities and first hyperpolarizability and the computed values have been converted into electrostatic units (esu) (α: 1 a.u = 0.1482x10^{-12} esu, β: 1 a.u = 8.6393x10^{-33} esu) [43,44].

Table 4 also contains the mean polarizabilities, α, and the anisotropy of polarizability Δα (molecules are in the xy plane). Compared to other applied methods, it is found that the B3LYP/6-311++G(d,p) level of theory leads in higher $\langle\alpha\rangle$. Furthermore, the mean polarizability is increased when a halogen atom or methyl group is added to the original molecules. This is because, in the case of derivatives, the molecular charge distribution is more susceptible to distortion by an external electric field than it is in the case of the original molecules. The calculated values of $\langle\alpha\rangle$ are 1.81 x 10^{-23} esu (B3LYP/6-311++G(d,p)), 1.81 x 10^{-23} esu (B3LYP/6-31+G(d,p)), 1.6 x 10^{-23} esu (HF/6-311++G(d,p)), 1.59 x 10^{-23} esu (HF/6-31+G(d,p)) for 2,3,4-CHMB. For 2,3,4-CHMB, the calculated values of anisotropy of the polarizability $\Delta\alpha$ are 1.34 x 10^{-23} esu (B3LYP), 1.06 x 10^{-23} esu (HF).

The values of first static hyperpolarizability with all components are shown in table 4. The values of β_{total} is 8.26x 10^{-30} esu with (B3LYP/6-311++G(d,p) for 2,3,4-CHMB. The standard molecule used to investigate the NLO characteristics of molecular systems is urea. As a result, urea was commonly used as a comparative threshold value. The computed values in this study are approximately 5–55 times that of urea (0.1947 × 10−30 esu). The high β value determined by the HF and B3LYP methods indicates that the compounds under study are high quality NLO materials. To calculate components of β theoretically is very useful because this clearly shows the direction of charge delocalization. Charge delocalization along the bond axis and the involvement of σ orbitals in the intramolecular charge transfer process are indicated by the smallest β_{zzz} value [42].

Electronic Spectra

Ultraviolet spectra of 2,3,4-CHMB have been studied both theoretically and experimentally. The UV–vis spectra of title compound was observed in various solvents (Acetone, Carbon Tetra Chloride and Diethyl Ether). TD-DFT has been used to identify the low-lying excited states of 2,3,4-CHMB with B3LYP/6-31+G(d,p) and B3LYP/6-311++G(d,p) based on a fully optimized ground-state structure. Calculations are carried out for excitation energies, oscillator strength (*f*) and wavelength (λ_{max}), and compared with observed experimental values. The computed values and experimental values of excitation energies, oscillator strength (*f*) and wavelength (λ_{max}), and spectral assignments are given in table 5. In the figure 3, the calculated and experimental UV/Vis spectra in various solvents are compared.

The ability to provide and accept electrons is characterized by the HOMO (Highest Occupied Molecular Orbital) and LUMO (Least Unoccupied Molecular Orbital) energies, respectively, while the molecular chemical stability is characterized by the

gap between both [42,45]. Since it measures electron conductivity, the energy gap between the HOMOs and LUMOs is a crucial factor in determining the electrical transport properties of molecules. For 2,3,4-CHMB, the energies of HOMO, LUMO, $HOMO_{-1}$ (Second Highest Occupied Molecular Orbital) and $LUMO_{+1}$ (Second Least Unoccupied Molecular Orbital) and energy gap between them in different solvents are calculated with the TD-DFT method and same basis sets and presented in tables 6 and 7.

In experimental UV-vis spectra of 2,3,4-CHMB, at wavelengths 318, 286 and 239 nm in acetone, at 307, 281 and 243 nm in carbon tetra chloride and at 311, 283 and 239 nm in diethyl ether solvents, the transitions are identified. Using B3LYP/6-31+G(d,p), the computed transitions were obtained at wavelengths of 318, 302, 262 nm in acetone, at 323, 298, and 261 nm in carbon tetra chloride, and at 320, 297, 258 nm in diethyl ether solvents. The transitions are obtained at wavelengths of 320, 303, and 263 nm in acetone solvent, 325, 299, and 262 nm in carbon tetra chloride solvent, and 322, 298, and 259 nm in diethyl ether solvent for the same compound at level B3LYP/6-311++G(d,p). There are three values of wavelengths, first wavelength corresponding to $n \rightarrow \pi^*$, another two corresponding to $\pi \rightarrow \pi^*$ transitions for each solvent [46, 47]. Solvents change the wavelength of transition for title compound. The most polar solvent is acetone and least polar CCl4 among these three solvents. Solvent effects: As the solvent's polarity increases, the $n \rightarrow \pi^*$ transition shifts to lower wavelength (blue shift) and $\pi \rightarrow \pi^*$ shifts to higher wavelength (red shift). When comparing the outcomes of the three solvents (tables 5-7), acetone has the lowest wavelength associated with the first transition, while CCl4 has the highest (i.e. shift towards lower wavelength on increasing the polarity of solvent). The values of the absorption maxima agree well with the theoretical values.

Table 1: Optimized geometrical parameters (bond lengths (A^0), bond angles (^{0}) and dihedral angles (^{0})) of 2,3,4-CHMB.

Parameters	6-31+G(d,p)		6-311++G(d,p)	
	HF	B3LYP	HF	B3LYP
Bond Length (A^0)				
C1-C2	1.401	1.412	1.400	1.408
C1-C6	1.384	1.401	1.382	1.398
C1-C9	1.489	1.483	1.490	1.483
C2-C3	1.379	1.394	1.377	1.391
C2-Cl12	1.738	1.752	1.739	1.752
C3-C4	1.401	1.412	1.399	1.409
C3-O13	1.341	1.357	1.340	1.354
C4-C5	1.381	1.396	1.379	1.393
C4-O15	1.348	1.366	1.346	1.364
C5-C6	1.387	1.392	1.385	1.389
C5-H7	1.072	1.083	1.072	1.081
C6-H8	1.073	1.085	1.073	1.083
C9-O10	1.193	1.221	1.187	1.214
C9-H11	1.087	1.103	1.088	1.103
O13-H14	0.946	0.970	0.943	0.967
O15-C16	1.408	1.429	1.406	1.428
C16-H17	1.079	1.090	1.079	1.088
C16-H18	1.084	1.096	1.085	1.094
C16-H19	1.084	1.096	1.085	1.094
Bond Angle (^{0})				
C2-C1-C6	118.7	118.6	118.6	118.6
C2-C1-C9	123.0	122.8	123.0	122.9
C1-C2-C3	120.9	120.8	121.0	120.9
C1-C2-Cl12	121.5	121.8	121.5	121.9
C6-C1-C9	118.3	118.5	118.4	118.5
C1-C6-C5	121.3	121.5	121.3	121.5
C1-C6-H8	118.4	117.7	118.4	117.7
C1-C9-O10	122.8	123.4	123.0	123.5
C1-C9-H11	116.8	116.2	116.5	116.0
C3-C2- Cl12	117.6	117.4	117.5	117.3
C2-C3-C4	119.2	119.1	119.2	119.1
C2-C3-O13	120.5	120.6	120.6	120.8
C4-C3- O13	120.2	120.2	120.2	120.2
C3-C4-C5	120.6	120.8	120.6	120.8
C3-C4-O15	113.8	113.3	113.8	113.3

C3-O13-H14	109.7	108.0	109.4	107.8
C5-C4-O15	125.6	125.9	125.6	125.9
C4-C5-C6	119.3	119.1	119.4	119.2
C4-C5-H7	120.9	120.8	120.9	120.8
C4-O15-C16	120.2	118.9	120.2	119.0
C6-C5-H7	119.7	120.1	119.7	120.1
C5-C6-H8	120.3	120.8	120.3	120.8
O10-C9-H11	121.4	120.3	120.5	120.5
O15-C16-H17	106.0	105.8	106.1	105.8
O15-C16-H18	110.9	110.8	110.9	110.9
O15-C16-H19	110.9	110.8	110.9	110.9
H17-C16-H18	109.5	109.7	109.4	109.6
H17-C16-H19	109.5	109.7	109.4	109.6
H18-C16-H19	110.0	110.0	109.9	110.0
Dihedral Angle (^{0})				
C6-C1-C2-C3	0.0	0.0	0.0	0.0
C6-C1-C2-Cl12	180.0	180.0	180.0	180.0
C9-C1-C2-C3	180.0	180.0	180.0	180.0
C9-C1-C2- Cl12	0.0	0.0	0.0	0.0
C2-C1-C6-C5	0.0	0.0	0.0	0.0
C2-C1-C6-H8	180.0	180.0	180.0	180.0
C9-C1-C6-C5	180.0	180.0	180.0	180.0
C9-C1-C6-H8	0.0	0.0	0.0	0.0
C2-C1-C9-O10	180.0	180.0	180.0	180.0
C2-C1-C9-H11	0.0	0.0	0.0	0.0
C6-C1-C9-O10	0.0	0.0	0.0	0.0
C6-C1-C9-H11	180.0	180.0	180.0	180.0
C1-C2-C3-C4	0.0	0.0	0.0	0.0
C1-C2-C3-O13	180.0	180.0	180.0	180.0
Cl12-C2-C3-C4	180.0	180.0	180.0	180.0
Cl12-C2-C3-O13	0.0	0.0	0.0	0.0
C2-C3-C4-C5	0.0	0.0	0.0	0.0
C2-C3-C4-O15	180.0	180.0	180.0	180.0
O13-C3-C4-C5	180.0	180.0	180.0	180.0
O13-C3-C4-O15	0.0	0.0	0.0	0.0
C2-C3-O13-H14	180.0	180.0	180.0	180.0
C4-C3-O13-H14	0.0	0.0	0.0	0.0
C3-C4-C5-C6	0.0	0.0	0.0	0.0
C3-C4-C5-C7	180.0	180.0	180.0	180.0
O15-C4-C5-C6	180.0	180.0	180.0	180.0
O15-C4-C5-H7	0.0	0.0	0.0	0.0
C3-C4-O15-H16	180.0	180.0	180.0	180.0
C5-C4-O15-H16	0.0	0.0	0.0	0.0
C4-C5-C6-C1	0.0	0.0	0.0	0.0
C4-C5-C6-H8	180.0	180.0	180.0	180.0
H7-C5-C6-C1	180.0	180.0	180.0	180.0
H7-C5-C6-H8	0.0	0.0	0.0	0.0
C4-O15-C16-H17	180.0	180.0	180.0	180.0
C4-O15-C16-H18	-61.22	-61.20	-61.22	-61.22
C4-O15-C16-H19	61.22	61.20	61.22	61.22

Table 2: The calculated thermodynamic parameters of 2,3,4-CHMB employing HF and B3LYP methods with 6-31+G(d,p) and 6-311++G(d,p) basis sets.

Thermodynamic Parameters (298 K)	6-31+G(d, p)		6-311++G(d, p)	
	HF	B3LYP	HF	B3LYP
Thermal Energy E_{Th} (kcal mol^{-1})				
Total	99.43	93.19	99.02	92.66
Electronic	0.00	0.00	0.00	0.00
Translational	0.89	0.89	0.89	0.89
Rotational	0.89	0.89	0.89	0.89
Vibrational	97.65	91.42	97.24	90.88
Heat Capacity at constt. Volume				
C_v (cal mol^{-1}K^{-1})				
Total	39.13	41.49	39.20	41.29
Electronic	0.00	0.00	0.00	0.00
Translational	2.98	2.98	2.98	2.98
Rotational	2.98	2.98	2.98	2.98
Vibrational	33.17	35.53	33.24	35.33
Entropy S (cal mol^{-1}K^{-1})				
Total	102.83	104.87	103.01	103.58
Electronic	0.00	0.00	0.00	0.00
Translational	41.57	41.57	41.57	41.57
Rotational	31.30	31.35	31.30	31.35
Vibrational	29.96	31.95	30.15	30.66
Zero-point Vibrational Energy				
E_{vib} (kcal/mol)	92.67	86.08	92.24	85.67
Rotational Constants (GHz)				
X	1.23	1.21	1.23	1.21
Y	0.62	0.61	0.62	0.61
Z	0.41	0.41	0.41	0.41

Table 3: The experimental thermodynamic parameters of 2,3,4-CHMB in Cal/Mol-K unit.

	2-Chloro-3-Hydroxy-4-Methoxybenzaldehyde			
Temperature	**Enthalpy**	**Heat capacity**	**Free Energy**	**Entropy**
K	**H**	**C_p**	**F**	**S**
200	11.53	20.69	-106.22	119.03
300	15.81	29.67	-111.70	129.13
400	20.23	38.19	-116.85	138.85
500	24.52	46.06	-121.83	148.23
600	28.55	53.12	-126.66	157.26
700	32.28	59.36	-131.34	165.93
800	35.72	64.83	-135.88	174.22
900	38.88	69.59	-140.27	182.14
1000	41.79	73.71	-144.52	189.69
1100	44.46	77.27	-148.63	196.88
1200	46.93	80.35	-152.61	203.74
1300	49.20	83.00	-156.45	210.28
1400	51.31	85.30	-160.18	216.52
1500	53.25	87.29	-163.79	222.47

Table 4: Nonlinear parameters (dipole moment, polarizability, and first-order hyperpolarizability) of 2,3,4-CHMB.

2-Chloro-3-Hydroxy-4-Methoxybenzaldehyde									
	Observed		Calculated						
			B3LYP/6-31+G(d,p)			B3LYP/6-311++G(d,p)			
Solvents	λ_{max}	**E**	λ_{max}	**E**	***f***	λ_{max}	**E**	***f***	**Assignments**
Acetone	318	3.90	318	3.90	0.00	320	3.87	0.00	$\pi \rightarrow \pi^*$
	286	4.34	302	4.11	0.12	303	4.10	0.11	$\pi \rightarrow \pi^*$
	239	5.19	262	4.73	0.29	263	4.71	0.29	$\pi \rightarrow \pi^*$
Diethyl Ether	311	3.99	320	3.88	0.00	322	3.85	0.00	$\pi \rightarrow \pi^*$
	283	4.39	297	4.17	0.08	298	4.16	0.08	$\pi \rightarrow \pi^*$
	239	5.19	258	4.81	0.22	259	4.79	0.23	$\pi \rightarrow \pi^*$
CCl_4	307	4.04	323	3.84	0.00	325	3.81	0.00	$\pi \rightarrow \pi^*$
	281	4.42	298	4.16	0.12	299	4.14	0.12	$\pi \rightarrow \pi^*$
	243	5.11	261	4.74	0.30	262	4.73	0.30	$\pi \rightarrow \pi^*$

Table 5: Electronic absorption spectra of 2,3,4-CHMB [absorption wavelength λ_{max} (nm), excitation energy (eV), and oscillator strength (*f*)] using TD-DFT with B3LYP/6-31+G(d,p) and B3LYP/6-311++G(d,p) basis sets.

Parameters	**6-31+G(d,p)**		**6-311++G(d,p)**	
	HF	**B3LYP**	**HF**	**B3LYP**
Dipole Moments				
(Debye)				
μ_x	3.09	3.51	3.05	3.44
μ_y	-4.89	-5.01	-4.87	-4.98
μ_z	0.00	0.00	0.00	0.00
μ_{Total}	5.79	6.11	5.75	6.05
Polarizability				
(a.u.)				
α_{xx}	126.50	147.62	127.06	147.35
α_{xy}	-10.96	-17.28	11.02	-17.19
α_{yy}	133.00	153.26	134.32	153.84
α_{xz}	000.00	000.00	000.00	000.00
α_{yz}	000.00	000.00	000.00	000.00
α_{zz}	61.41	65.00	62.26	65.49
$\langle\alpha\rangle$ (esu)	1.59×10^{-23}	1.81×10^{-23}	1.6×10^{-23}	1.81×10^{-23}
$\Delta\alpha$ (esu)	1.06×10^{-23}	1.34×10^{-23}	1.06×10^{-23}	1.34×10^{-23}
Hyperpolarizability				
(a.u.)				
β_{xxx}	238.95	-516.83	-224.89	-496.07
β_{xxy}	172.36	329.33	168.42	325.77
β_{xyy}	-220.80	-404.41	-211.79	-393.13
β_{yyy}	-14.68	32.68	-28.24	0.65
β_{xxz}	0.00	0.00	0.00	0.00
β_{xyz}	0.00	0.00	0.00	0.00
β_{yyz}	0.00	0.00	0.00	0.00
β_{xzz}	-39.68	-37.51	-32.82	-28.73

β_{yzz}	-36.40	-46.96	-43.33	-59.55
β_{zzz}	0.00	0.00	0.00	0.00
β_x	-21.52	-958.75	-469.50	-917.93
β_y	121.27	315.05	96.85	266.87
β_z	0.00	0.00	0.00	0.00
(esu) β_{Total}	1.06 x 10^{-30}	8.72 x 10^{-30}	4.14 x 10^{-30}	8.26 x 10^{-30}

Table 6: Calculated Energy values (eV) of 2,3,4-CHMB by using TD-DFT/B3LYP/6-31+G(d,p).

Solvents	E_{HOMO}	E_{LUMO}	E_{HOMO-1}	E_{LUMO+1}	ΔE	∂E	E_{Total}(Hartree)
Acetone	-6.71	-2.01	-7.20	-0.52	4.70	6.68	-994.94
Diethyl	-6.74	-2.02	-7.22	-0.57	4.72	6.65	-994.94
Ether							
CCl_4	-6.77	-2.02	-7.24	-0.61	4.76	6.63	-994.94

ΔE=E_{LUMO} - E_{HOMO}, ∂E=E_{LUMO+1} - E_{HOMO-1}

Table 7: Calculated Energy values (eV) of 2,3,4-CHMB by using TD-DFT/B3LYP/6-311++G(d,p).

Solvents	E_{HOMO}	E_{LUMO}	E_{HOMO-1}	E_{LUMO+1}	ΔE	∂E	E_{Total} (Hartree)
Acetone	-6.77	-2.08	-7.25	-0.62	4.69	6.63	-995.09
Diethyl	-6.80	-2.08	-7.27	-0.66	4.72	6.61	-995.09
Ether							
CCl_4	-6.83	-2.08	-7.28	-0.70	4.75	6.58	-995.09

ΔE=E_{LUMO} - E_{HOMO}, ∂E=E_{LUMO+1} - E_{HOMO-1}

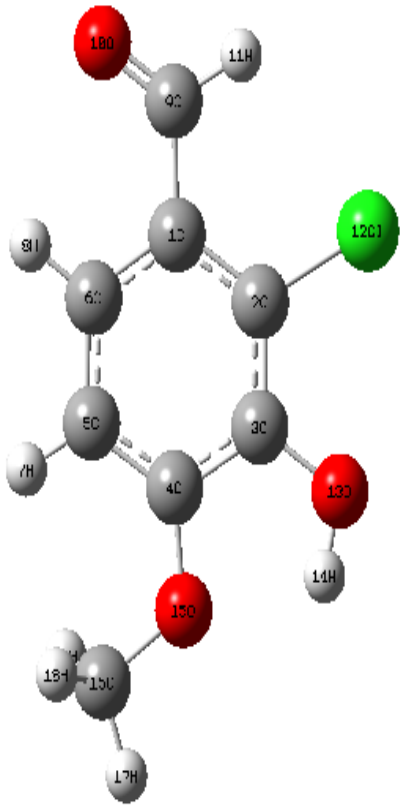

Fig 1: The optimized geometric structure with atoms numbering of 2-Chloro-3-Hydroxy-4-methoxybenzaldehyde.

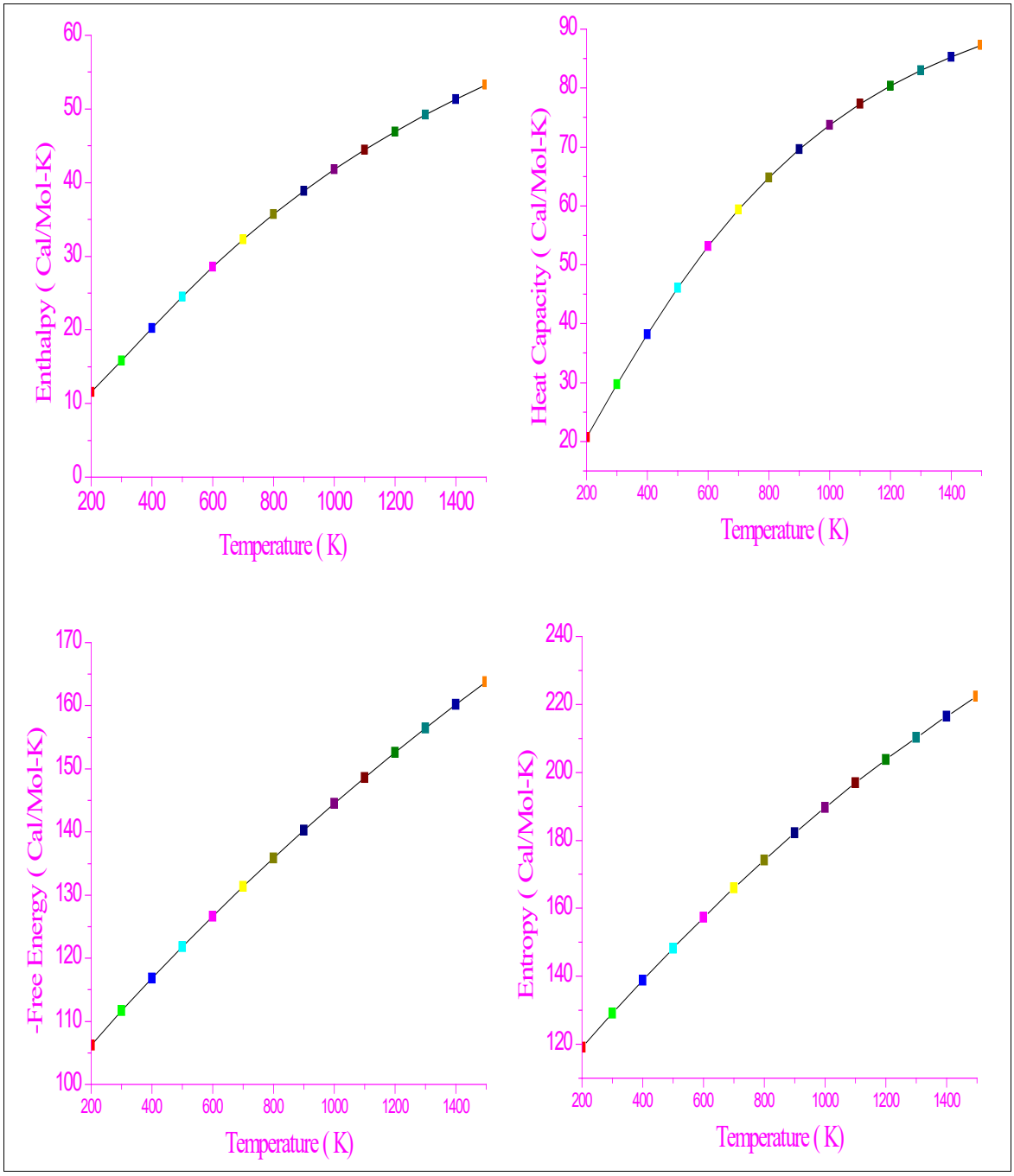

Fig 2: The graph of thermodynamic functions and temperature of 2, 3,4-CHMB.

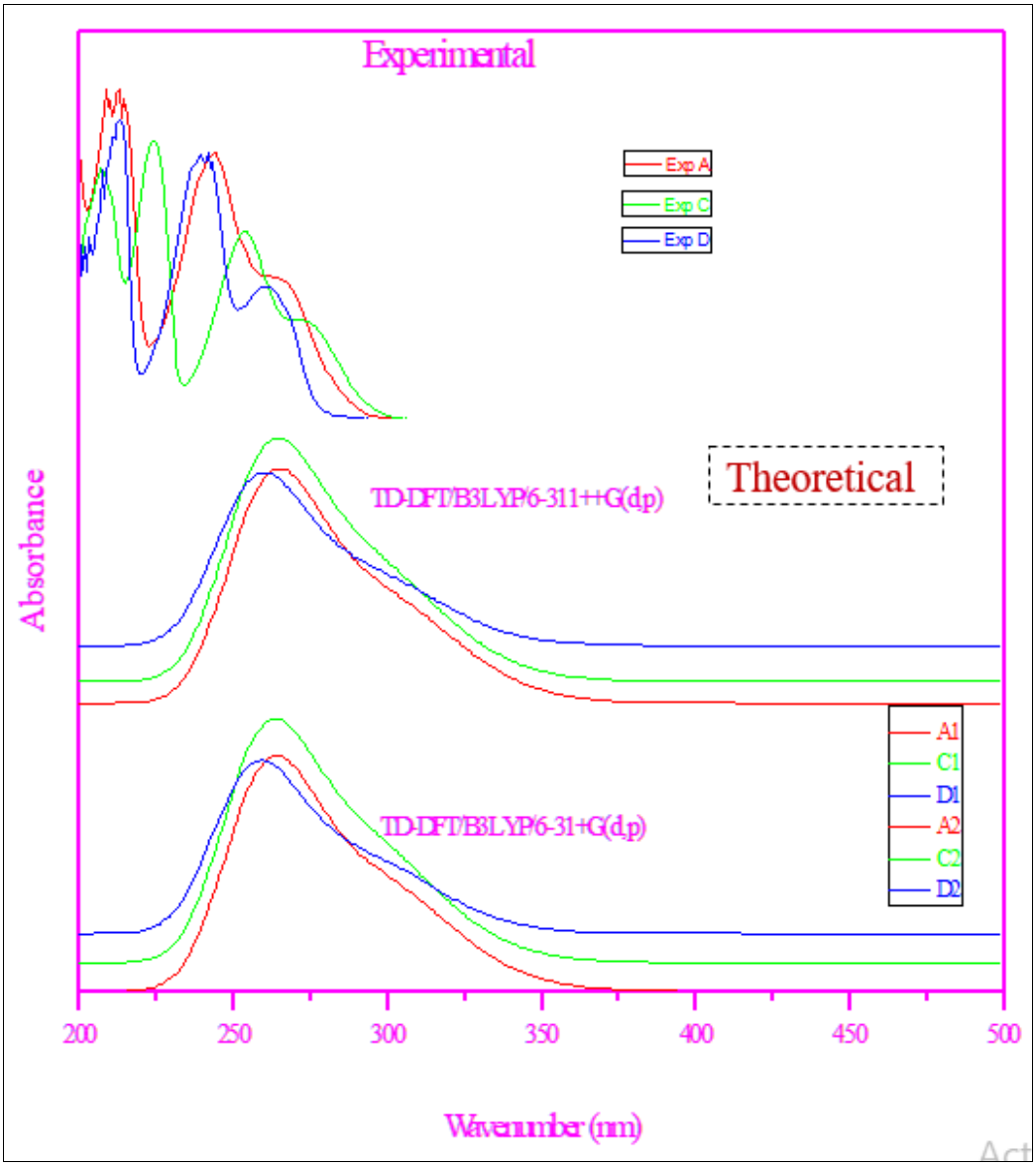

Fig 3: Experimental and Theoretical UV/Vis Spectra of 2,3,4-CHMB in different solvents.
A- Acetone, C-Carbon Tetra Chloride, D-Diethyl Ether

Conclusion

In this work, an attempt has been made to study the UV-vis spectral studies, NLO properties, and thermodynamic properties at different temperatures of the industrially significant 2,3,4-CHMB both theoretically and experimentally. At HF and DFT/B3LYP, equilibrium geometries, electronic parameters, and thermodynamic parameters of 2,3,4-CHMB have been studied with the basis sets 6-311G++(d,p) and 6-31+G(d,p). The relationships between temperature and thermodynamic parameters demonstrate that as temperature rises, so do heat capacities, entropies, and enthalpies because of the increased intensity of molecular vibrations. The molecule's electronic structures and properties were profoundly revealed by the TD-DFT calculations. Moreover, the thermodynamic functions and computed UV-Vis results agree significantly with the experimental data. The molecule's bioactive properties are supported by the reduction of the HOMO–LUMO band gap. The title compound is a strong contender for a nonlinear optical material, as indicated by the anticipated NLO properties. Future research on nonlinear optics will find the computed first hyperpolarizability to be an interesting object, as it is comparable to the reported values of similar derivatives.

References

1. Hiremath, Jayashree Yenagi CS, Tonannavar J. Spectrochimica Acta Part A, 2007, 68:710-717.
2. Silverstein RM, Webster FX. "Spectrometric Identification of Organic Compounds", 6th Edition, John Wiley, Asia, 2003.
3. Bednarek P, Bally T, Gebicki J. J. Org. Chem. 2002; 67:1319.
4. Hiremath CS, Tonannavar J. Spectrochim. Acta A. 2009; 73:388-397.
5. http://www.faizkaskar.8k.com/applications.html.
6. Sajan D, Hubert Joe I, Jayakumar VS, Zaleski J. J. Mol. Struct. 2006; 785:43-53.
7. Singh DN, Singh ID, Yadav RA. *Ind. J. Phys.* 2002; 76(3):307-318.
8. Ribeiro-Claro PJA, Marques MPM, Amado AM. Chem., Phys., Chem. 2002; 3:599.
9. Qayyum MD, Venkatram Reddy B, Ramana Rao G. Spectrochimica Acta A. 2004; 60:279.
10. Itoh T, Akai N, Ohno K. J. Mol. Struct. 2006; 786:39.
11. Hirematha CS. Tom Sundius, Spectrochimica Acta Part A. 2009; 74:1260-1267.

12. Aralakkanavar MK, Katti NR, Jeeragal PR, Kalakoti GB, Rao R, Shashidhar MA. Spectrochimica Acta A. 1992; 48:983.
13. Yadav RA, Singh IS. Ind. J. Phys. 58B. 1984; (6):556-569.
14. Riahi S, Bayandori Moghaddam A, Ganjali MR, Norouzi P, Latifi M, J. Mol. Struct. (THEOCHEM). 2007; 807:137-145.
15. Riahi S, Ganjali MR, Moghaddam AB, Norouzi P, Spectrochimica Acta Part A. 2008; 70:94-98.
16. Jenepha Mary SJ, C. James Quantum chemical insight into molecular structure, Chemical Data Collections. 2020; 29:100530.
17. Park S, Kim DS, Kang S, Eur. J. Nutr. 50, 2011, 107-118.
18. Kenawy ER, Worley SD, Broughton R. Biomacromolecules. 2007; 8:1359-1384.
19. Park ES, Moon WS, Song MJ, Kim MN, Chung KH, Yoon DS. Int. Biodeter. Biodegr. 2001; 47:209-214.
20. D Jayareshmi H, Marshan Robert D. Aruldhas, Elucidation of the structure, spectroscopic techniques, and quantum chemical investigations on nonlinear optical material 2–hydroxy-5-methylbenzaldehyde, Journal of Molecular Structure. 2021; 1238:130426.
21. Sundaraganesan N, Ilakiamani S, Dominic Joshua B, Spectrochimica Acta Part A. 2007; 68:680-687.
22. Krishnakumar V, Balachandran V. Spectrochimica Acta Part A. 2006; 63:464-476.
23. Sajan D, Binoy J, Pradeep B, Venkatakrishnan K, Kartha VB, Joe IH, Jayakumar VS. Spectrochimica Acta. 2004; 60:173-180.
24. Dr. Kanis, Ratner MA, Marks TJ. Chem. Rev. 1994; 94:195–242.
25. Williams DJ. "Introduction to Nonlinear Optical Effects in Molecules and Polymers", Wiley, New York, 1991.
26. Frisch MJ. *et al.* Gaussian 09 program, Revision A Gaussian, Inc., Wallingford CT, 2009, 02.
27. Durig JR, Little TS, Gounev TK, Gargner Jr. JK, Sullivan JF. J. Mol. Struct. 1996; 375:83.
28. Karabacak M, Karagoz D, Kurt M. J. Mol. Struct. 2008; 892:25-31.
29. Karabacak M, Kurt M, Atac A. J. Phys. Org. Chem. 2009; 22:321-330.
30. Hermetet AK, Ackerman JL, Eilts KK, Johnson TK, Swearingen JK, Giesen JM. *et al*. J. Mol. Struct. 2002; 605:241.
31. Karabacak M, Cinar M, Kurt M. J. Mol. Struct. 2008; 885:28-35.
32. Rai AK, Kumar S, Rai A, Spectrosc VIB. 2006; 42:397-402.
33. Karabacak M, Kurt M. Spectrochimica Acta A. 2008; 71:876-883.
34. Rai AK, Kumar S. A. Rai, Vibrational Spectroscopy. 2006; 42:397-402.
35. www.chemcraft.com.
36. Mcquarrie DA. "Statistical Thermodynamics", (Harper and Row Publishers, New York)**,** 1973.
37. Strekalov ML. Chemical Physics. 2009; 355:62-66.
38. Irikura KK, Frurip DJ. Computational Thermochemistry-Prediction and Estimatoin of Molecular Thermodynamics, American Chemical Society, Washington, DC, 1998.
39. John M, Seddon, Julian D. Gale, Thermodynamics and Statistical Mechanics", (Royal Society of Chemistry, London), 2001, 98.
40. Mehmet Karabacak, Leena Sinha,Onkar Prasad,, Zeliha Cinar, Mehmet Cinar, Spectrochimica Acta Part A. 2012; 93:33-46.
41. Govindarajan M, Karabacak M, Udayakumar V, Periandy S. Spectrochimica Acta Part A. 2012; 89:137-148.
42. Mehmet Karabacak, Etem Kose. Ahmet Atac, Spectrochimica Acta Part A. 2012; 91:83-96.
43. Asghari-Khiavi M, Hojati-Talemi P, Safinejad F. Journal of Molecular Structure: THEOCHEM, 2009; 910:56-60.
44. Singh RN, Amit Kumar RK. Tiwari, Poonam Rawat, Vikas Baboo, Divya Verma, Spectrochimica Acta Part A. 2012; 92:295-304.
45. Fukui K. Science. 1982; 218:747-754.
46. Nobuyuki Akai, Satoshi Kudoh, Masao Takayanagi, Munetaka Nakata. Journal of Photochemistry and Photobiology A: Chemistry. 2002; 150:93-100.
47. Rajendiran N, Balasubramanian T. Spectrochimica Acta Part A. 2008; 69:822-829.